

Analysis of the diffractively produced $\pi^- \pi^- \pi^+$ final state at COMPASS

F. Markus Kaspar and S. Gerassimov for the COMPASS Collaboration

Physik-Department E18, Technische Universität München, 85748 Garching, Germany.

Received 14 January 2022; accepted 18 February 2022

The COMPASS experiment at CERN collected a large sample of diffractively produced $\pi^- \pi^- \pi^+$ events. The data contain contributions from light-meson resonances with the quantum numbers of π_{J^-} - and a_{J^-} -like states. We performed a partial-wave analysis of this final state for proton and nuclear targets. We consistently observe a π -like signal with $J^{PC} = 0^{-+}$ in the $f_2(1270)\pi D$ wave. The signal appears to be incompatible with the established $\pi(1800)$ resonance, which we observe in the decays into $(\pi\pi)_S \pi S$, $f_0(980)\pi S$ and $f_0(1500)\pi S$ waves.

Keywords: COMPASS; partial-wave analysis; PWA; $\pi(1800)$; hybrid; diffraction; light mesons; resonance; meson spectroscopy.

DOI: <https://doi.org/10.31349/SuplRevMexFis.3.0308020>

1. Introduction

The study of the meson spectrum helps us to better understand QCD in the non-perturbative regime. In recent times more and more involved analyses, both of experimental data and simulations in the form of lattice QCD, have become possible. Particularly the search for states that are not predicted by the quark model, *i.e.* glueballs and hybrid states, has been of great interest. While some of these states can be distinguished from classical states based on their quantum numbers which are forbidden in the quark model, so-called exotic states, others require detailed analyses of their decays. Hints for such a non-exotic hybrid state were observed by the VES Collaboration in Refs. [1, 2]. There seems to be an additional lower-lying π -like state as compared to the well-established $\pi(1800)$ resonance (see Ref. [3]). This might point to a possible hybrid character of the $\pi(1800)$ according to Ref. [4] and references therein.

The COMPASS experiment collected a large sample of diffractively produced $\pi^- \pi^- \pi^+$ events for different target types. The data contain contributions from isovector π_{J^-} - and a_{J^-} -like meson resonances, thereby giving us access to the same signal as observed by VES. We model the diffractive reaction according to the diagram shown in Fig. 1. The three-pion resonance X^- is produced in the excitation of the 190 GeV/c π^- beam during the interaction with the target.

In the following we present the results of our ongoing analysis of π -like signals.

2. Data Sets

COMPASS recorded data for a (light) proton target in the form of liquid hydrogen $l\text{H}_2$ as well as for (heavy) solid state targets made of Nickel (Ni) and Lead (Pb). For the liquid hydrogen target we now use the full COMPASS data set and perform an improved event selection as compared to Ref. [5]. We obtain a data set of $115 \cdot 10^6$ exclusive $\pi^- \pi^- \pi^+$ events in the kinematic region $0.5 < m_{3\pi} < 2.5$ GeV/c² and $0.1 < t' < 1.0$ (GeV/c²) with t' being the reduced squared four-momentum transfer² defined in Eq. (6) in Ref. [5], which

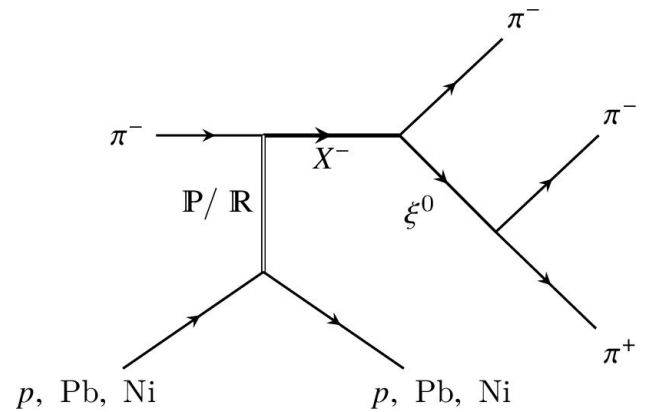


FIGURE 1. Diffractive dissociation reaction with Pomeron (P) and Reggeon (R) exchange respectively. The target stays intact and the beam π^- is excited to a resonance X^- . We assume the isobar model, *i.e.* that the X^- decays into a bachelor pion π^- and a $\pi^- \pi^+$ resonance ξ^0 , the so-called isobar.

takes into account the minimum momentum transfer required to excite the resonance X^- . We are able to more than double our available events for the light target as compared to the previous analysis published in Refs. [5, 6]. Figure 2a) shows the three-pion mass spectrum with clear indication of the well-known $a_2(1320)$ and $\pi_2(1670)$ resonances (see Ref. [3]). The heavy target data contain $13.5 \cdot 10^6$ events for the Pb target and $12.5 \cdot 10^6$ events for the Ni target in the same mass range and in $0.0 < t' < 1.5$ (GeV/c²). Due to the faster decaying form factor of the heavy nuclei the Pb and Ni data are more concentrated at low t' , therefore effectively extending our analysis into this kinematic region.

3. Partial-Wave decomposition

We perform a partial-wave analysis (PWA) of the data. We follow the same approach as described in Ref. [5] and use the same PWA model with 88 waves. We model the decay of the X^- resonance with spin J and parity P using the isobar model, *i.e.* we assume that the X^- first decays into a $\pi\pi$ resonance ξ^0 , the isobar, and a so-called bachelor pion with orbital angular momentum L between them. We assign the

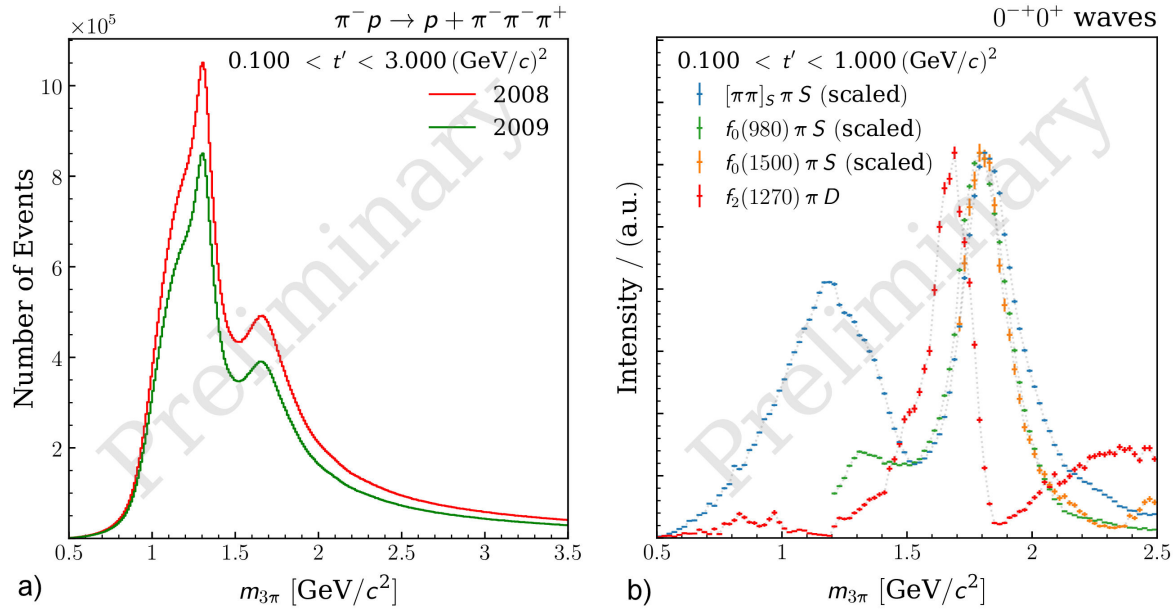


FIGURE 2. a) 3π invariant mass distribution for the lH_2 data from the 2008 (red) and 2009 (green) COMPASS data-taking campaigns. The two dominant resonances, $a_2(1320)$ and $\pi_2(1670)$, are visible as peaks. b) Comparison of the intensity distribution of four selected 0^{-+} waves. The $0^{-+}0^+ f_2(1270)\pi D$ wave in red is shifted towards lower masses compared to the three $0^{-+}0^+ \pi S$ waves. The $m_{3\pi}$ spectrum a) shows dominant resonances. The contributions of individual quantum numbers can be extracted using a partial-wave decomposition. Results for selected waves are shown in b).

charge parity C of the neutral partner resonance to X^- . M denotes its spin projection and ϵ the reflectively quantum number, see Ref. [5]. Each partial wave is therefore labelled by $J^{PC} M^\epsilon \xi^0 \pi L$. The $m_{3\pi}$ and t' dependence of the partial-wave amplitudes is unknown. We therefore bin our data in $m_{3\pi}$ and t' and perform the partial-wave decomposition independently for each kinematic bin. As a result, we obtain a set $\{T_i\}$ of complex valued transition amplitudes for each bin, thereby extracting the $m_{3\pi}$ and t' dependence of every partial-wave amplitude in a quasi-model-independent way. Each transition amplitude encodes the intensity $|T_i|^2$ and relative phase $\arg T_i$ with respect to an anchor wave with a real valued amplitude. Figure 2b) shows the intensity spectrum of four selected $J^{PC} = 0^{-+}$ waves summed over t' obtained from the partial-wave decomposition for the liquid hydrogen data. The three waves decaying into $J^{PC} = 0^{++}$ isobars all show a nearly identical peak around $1.8 \text{ GeV}/c^2$, which corresponds to the established $\pi(1800)$ resonance. In contrast to this, the signal in the $0^{-+}0^+ f_2(1270)\pi D$ wave is shifted towards lower masses, with an intensity peak around $1.7 \text{ GeV}/c^2$. For COMPASS data, this has first been observed in the analysis of the 2008 data set in Ref. [7] and could now be confirmed and improved with the full data set. We observe the same behavior in the heavy target analysis. The comparison in Fig. 3a) shows the intensity of $0^{-+}0^+ f_2(1270)\pi D$ wave summed over t' . The Pb result in green has been scaled to the intensity peak of the lH_2 results. The peak shapes match perfectly for both data sets. The same signal has been observed by the VES Collaboration (see Fig. 4d) in Ref. [1]).

However, a resonance signal not only consists of an in-

tensity peak but also of a corresponding rapid phase motion. In Fig. 3b), we compare the relative phase between the $0^{-+}0^+ f_2(1270)\pi D$ and the $4^{++}1^+ \rho(770)\pi G$ wave for selected t' bins of the different target types. Indeed, the phase rises from approximately $1.3 \text{ GeV}/c^2$ and to $1.8 \text{ GeV}/c^2$, providing further evidence for resonant behavior.

4. Resonance-Model fit

To study the resonance content of the partial-wave amplitudes, we model their $m_{3\pi}$ dependence using the same method as described in Ref. [6]. We select seven partial waves and fit their measured intensities and all their relative

TABLE I. Seven-wave resonance model: Each wave is described by a resonant Breit-Wigner amplitude and a non-resonant background term with the equation given in Ref. [6]. The last column is the fitted $m_{3\pi}$ range.

Partial wave	Resonance	Non-res.	$m_{3\pi}$ range [GeV/c ²]
$0^{-+}0^+ [\pi\pi]_S \pi S$	$\pi(1800)$	Eq. (29)	1.60 to 2.30
$0^{-+}0^+ f_0(980)\pi S$	$\pi(1800)$	Eq. (29)	1.20 to 2.30
$0^{-+}0^+ f_0(1500)\pi S$	$\pi(1800)$	Eq. (29)	1.70 to 2.30
$0^{-+}0^+ f_2(1270)\pi D$	$\pi(1700)$	Eq. (29)	1.30 to 2.30
$1^{++}0^+ f_0(980)\pi P$	$a_1(1420)$	Eq. (29)	1.30 to 1.70
$2^{++}1^+ \rho(770)\pi D$	$a_2(1320)$	Eq. (27)	0.90 to 2.00
$4^{++}1^+ \rho(770)\pi G$	$a_4(1970)$	Eq. (29)	1.25 to 2.30

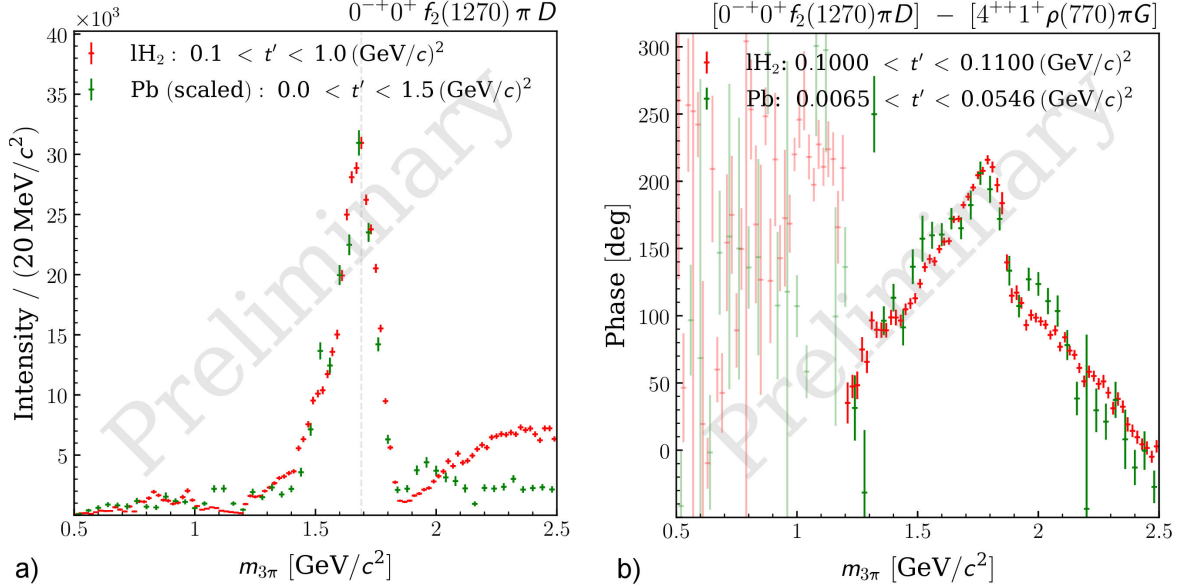


FIGURE 3. Comparison of the intensity summed over t' a) and phase-motion of the $0^{-+}f_2(1270)\pi D$ wave with respect to the $4^{++}\rho(770)\pi G$ wave for to selected t' -bins b). In red is the result for the lH_2 target and in green for the Pb target.

phases simultaneously with the resonance model summarized in Table I. Each amplitude is described as the coherent sum of resonant Breit-Wigner amplitudes and non-resonant terms to describe background contributions. The 0^{-+} waves with 0^{++} isobars are all fitted with the same $\pi(1800)$ resonance. The 1^{++} , 2^{++} and 4^{++} waves are included to constrain the fit via the additional relative phases.

We attempt to describe the peak in the $0^{-+}f_2(1270)\pi D$ wave with different models. In Table I we denote this component $\pi(1700)$ to indicate that we use a separate Breit-Wigner in this case. Overall we use five different resonances to describe the seven waves. We obtain the resonance parameters given in Table II for the lH_2 target and in Table II for the Pb target. We do not provide uncertainties, as they are dominated by systematic effects, which require extensive studies, as have been performed for the results in Ref. [5]. We observe a lower resonance mass and a smaller width for the $\pi(1700)$ component as compared to the $\pi(1800)$ in both data samples. The deviation is stronger for the Pb-target data, which we assume to be due to different background contributions for the

TABLE II. Resonance parameters for the lH_2 -target data (left) and Pb-target data (right).

Resonance	Mass [MeV/c ²]	Width [MeV/c ²]	Mass [MeV/c ²]	Width [MeV/c ²]
$\pi(1700)$	1740	171	1698	157
$\pi(1800)$	1795	230	1781	221
$a_1(1420)$	1414	149	1414	166
$a_2(1320)$	1316	115	1318	102
$a_4(1970)$	1939	395	1988	322

different targets. Above approximately 1.9 GeV/c² a shoulder in the intensity spectrum is visible in the lH_2 -target data. We assume this is background and we elaborate in the next section.

5. Systematic Studies

We performed a first set of systematic studies on the lH_2 -target data. We tried four different resonance models. First, we tried to describe the peak in the $0^{-+}f_2(1270)\pi D$ wave with the $\pi(1800)$ resonance, using the same Breit-Wigner parameters as for the other $0^{-+}0^{+}$ waves. With this approach we are unable to get a satisfactory description of the intensity peak of the $0^{-+}0^{+}f_2(1270)\pi D$ wave. We also attempted to describe it using only a non-resonant background term, which fails to describe the data, as expected. Following the fit studies in Ref. [7], we tried to describe the $0^{-+}0^{+}f_2(1270)\pi D$ wave using two resonances, either using the $\pi(1800)$ and an additional free resonance or using two free resonances. While these models are in principle able to describe the data, we find the same behavior as described in Ref. [7], *i.e.* one of the resonances is used as a broad effective background component. We consider these solutions of two strongly overlapping Breit-Wigners to be unphysical. The best description of the data is therefore achieved with a separate $\pi(1700)$ resonance for the $f_2(1270)\pi D$ wave.

We have also investigated the effect of the PWA model. The high-mass shoulder in the intensity spectrum of the lH_2 -target data seems to be sensitive to the wave set used in the partial-wave decomposition. Using larger wavesets decreases the intensity of the shoulder, making the intensity distribution more similar to that of the heavy-target data. A similar effect can be observed with the inclusion of coherent background

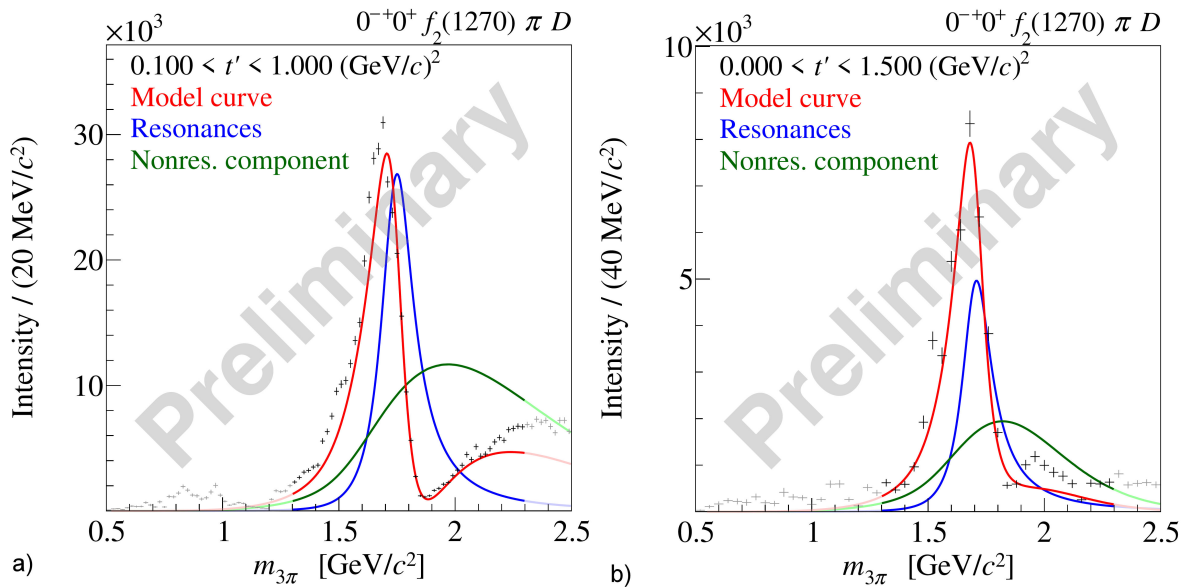


FIGURE 4. Intensity distribution of the $0^{-+}f_2(1270)\pi D$ wave summed over t' . The resonance-model fit (red) of the coherent sum of a $\pi(1700)$ Breit-Wigner amplitude (blue) and a background term (green) is able to describe the data (black data points with statistical uncertainties). a) H_2 target data; b) Pb target data.

models for the Deck effect (Ref. [8]) and central production (see *e.g.* Sec. 2.4 of Ref. [9]) into the partial-wave decomposition. We therefore assume that the shoulder is indeed due to coherent background. Further studies will show whether the resonance-model fits for both target types will produce more similar results.

6. Interpretation

We do observe clear resonant behavior in the $1.7 \text{ GeV}/c^2$ region of the $0^{-+}0^+f_2(1270)\pi D$ wave. Several different interpretations are possible. Conservatively, one could assume that a more complicated background description is required and that the signal indeed originates from interference of the $\pi(1800)$ and background. Following the arguments presented by the authors of Ref. [4], which were also pointed out in Refs. [2, 7], the observation of a preferred decay of the $\pi(1800)$ into 0^{++} isobars could indicate that it is in fact a hybrid state and that the signal observed in the $0^{-+}0^+f_2(1270)\pi D$ wave originates from the conventional quark-model state. However, in this case also a combination of two resonances has to be taken into account. This would require a more sophisticated resonance model in order to correctly take into account the overlapping resonances.

7. Conclusion and outlook

We observe a resonance signal in the $0^{-+}f_2(1270)\pi D$ wave with an intensity peak and an associated rapid phase mo-

tion, which are clearly visible in both heavy and light-target data. The amplitude of this wave is not well described by the $\pi(1800)$ resonance. The simplest model that describes the data contains a separate Breit-Wigner resonance at a lower mass of about $1.7 \text{ GeV}/c^2$. The same signal has been observed by the VES Experiment in the $\pi^-\pi^-\pi^+$ and $\omega\rho$ channels. We are currently working on systematic studies of both the partial-wave decomposition and the resonance-model fit in order to estimate systematic uncertainties. The COMPASS diffractive data also contain $\omega\rho$ decays. An upcoming analysis of this channel can help to further complement the current results of this analysis and the VES results.

Acknowledgements

We thank our colleagues at TUM and CERN, especially S. Paul, B. Grube, S. Wallner, D. Ryabchikov and A. Maltsev for their help and support. F. Kaspar also thanks S. Steinbeißer for their general discussions.

This research is part of the Blue Waters sustained-petascale computing project, which is supported by the National Science Foundation (awards OCI-0725070 and ACI-1238993) and the state of Illinois. Blue Waters is a joint effort of the University of Illinois at Urbana-Champaign and its National Center for Supercomputing Applications. This work is also part of the ‘‘Mapping Proton Quark Structure using Petabytes of COMPASS Data’’ PRAC allocation supported by the National Science Foundation (award number OCI-1713684).

- i.* Here $\|t'\| \approx \|t\|$.
1. D. V. Amelin et al. [VES Collaboration], Study of resonance production in diffractive reaction $\pi^- A \rightarrow \pi^+ \pi^- \pi^- A$, *Phys. Lett. B* **356** (1995) 595, [https://doi.org/10.1016/0370-2693\(95\)00864-H](https://doi.org/10.1016/0370-2693(95)00864-H)
 2. D. V. Amelin et al. [VES Collaboration], Study of the reaction $\pi^- Be \rightarrow \omega \pi^- \pi^0 Be$, arXiv (1998), preprint available at <https://arxiv.org/abs/hep-ex/9810013>
 3. P. A. Zyla et al. [Particle Data Group], *Review of Particle Physics* **2020** (2020) 083C01, <https://doi.org/10.1093/ptep/ptaa104>
 4. F. E. Close and P. R. Page, Distinguishing hybrids from radial quarkonia, *Phys. Rev. D* **56** (1997) 1584, <https://link.aps.org/doi/10.1103/PhysRevD.56.1584>
 5. C. Adolph et al. [COMPASS Collaboration], Resonance production and $\pi\pi$ S -wave in $\pi^- + p \rightarrow \pi^- \pi^- \pi^+ + p_{\text{recoil}}$ at 190 GeV/ c , *Phys. Rev. D* **95** (2017) 032004, <https://link.aps.org/doi/10.1103/PhysRevD.95.032004>
 6. M. Aghasyan et al. [COMPASS Collaboration], Light isovector resonances in $\pi^- p \rightarrow \pi^- \pi^- \pi^+ p$ at 190 GeV/ c , *Phys. Rev. D* **98** (2018) 092003, <https://link.aps.org/doi/10.1103/PhysRevD.98.092003>
 7. F. Haas, Two-Dimensional Partial-Wave Analysis of Exclusive 190 GeV $\pi^- p$ Scattering into the $\pi^- \pi^- \pi^+$ Final State at COMPASS (CERN), PhD thesis (2014), <http://cds.cern.ch/record/1662589/>
 8. R. T. Deck, Kinematical Interpretation of the First $\pi - p$ Resonance, *Phys. Rev. Lett.* **13** (1964) 169, <https://link.aps.org/doi/10.1103/PhysRevLett.13.169>
 9. A. B. Kaidalov, Diffractive production mechanisms, *Physics Reports* **50** (1979) 157, [https://doi.org/10.1016/0370-1573\(79\)90043-7](https://doi.org/10.1016/0370-1573(79)90043-7)